Proc. of the 8th International Symposium on Geotechnical Safety and Risk (ISGSR)
Edited by Jinsong Huang, D.V. Griffiths, Shui-Hua Jiang, Anna Giacomini and Richard Kelly
 Published by Research Publishing, Singapore.
doi: 10.3850/978-981-18-5182-7_04-003-cd

Probabilistic Analysis of an Anchored Diaphragm Wall installed in Normally Consolidated Sands

Marek Kawa[1], Wojciech Puła[2] and Andrzej Truty[3]

[1]Faculty of Civil Engineering, Wroclaw University of Science and Technology,
Wyb. Wyspianskiego 27, 50-370 Wroclaw, Poland
E-mail: marek.kawa@pwr.edu.pl
[2]Faculty of Civil Engineering, Wroclaw University of Science and Technology,
Wyb. Wyspianskiego 27, 50-370 Wroclaw, Poland
E-mail: wojciech.pula@pwr.edu.pl
[3]Faculty of Civil Engineering, Cracow University of Technology,
Warszawska 24, 31-155 Cracow, Poland
E-mail: andrzej.truty@pk.edu.pl

Abstract:
This paper deals with the probabilistic modelling of a triple-anchored diaphragm wall. The analysis is carried out using random finite element method based on N=1000 Monte Carlo simulations. Single spatially variable soil layer described by two random fields modelling normalized CPTu parameters Q_{tn} and F_r is assumed. The probability distribution, cross-correlation coefficient and vertical SOF for both random fields are identified based on CPTu tests of normally consolidated sand from central part of Poland. The Hardening Soil-Brick model is adopted for the soil medium and its parameters are derived based on local Q_{tn} and F_r values. The paper presents the obtained probability characteristics of the results, namely: maximum displacement of the wall, maximum bending moment in the wall and value of force in the upper anchor.

Keywords: Random field; scale of fluctuation; random finite element analysis; anchored diaphragm walls; sands

1 Introduction

In recent decades, in civil engineering there has been a growing interest in estimating the probability of structural failure and in the related problem of so-called reliability based design. In geotechnics the spatial variability of soil parameters is considered to be the main risk factor (Fenton & Griffiths, 2008). It is becoming common practice to model this variability using stationary random field. In the engineering practice stationary random field is usually described by point probability distribution of modelled parameter and its spatial autocorrelation function or more specifically its parameters, so-called scales of fluctuations (SOFs).
One of the most popular approaches of including random fields in the description of a soil medium is the random finite element method (RFEM, Griffiths and Fenton 1993, Fenton and Griffiths 2008). The method involves generating an appropriate number of realisations of random fields describing soil parameters, mapping the generated realisations into the finite elements describing the soil in a given boundary problem mesh, and then solving the resulting Monte-Carlo simulations. The method is very universal. To date, it was used for probabilistic modelling of foundations (eg. Fenton & Griffiths, 2003; Kawa and Puła, 2020), slopes (eg. Griffiths & Fenton, 2004), and many other structures.
Among geotechnical structures, due to the significant consequences of failure, reliability analysis should include large retaining walls. In case of these structure often serviceability limit state is a factor deciding about their failure. Displacement and internal forces of these structures can strongly be influenced by the stiffness behaviour of the adjacent soil. For that reason, for engineering modelling of these structures more advanced soil models including the non-linear behaviour of the soil in elastic range are nowadays increasingly used. One of the more adequate models is the Hardening Soil-Brick model verified experimentally on displacements of an anchored wall in the Berlin sand benchmark (Schweiger 2002) Recently, the model has also been applied (in conjunction with RFEM) to assess the reliability of the anchored and cantilever walls (Sert et al. 2016., Luo et al. 2018, Kawa et al., 2021).
A common problem with RFEM, in which usually only soil strength parameters are modelled with random fields, is the lack of satisfactory estimations of these parameters probability distributions. Of the tests which provide satisfactory number of results to estimate such distribution (and/or SOF), CPTu seem to be adequate. However, it does not directly test cohesion c or the angle of internal friction ϕ, and the relationships between the registered cone resistance q_c or sleeve friction f_s tested by CPTu and c and ϕ are not always well defined. On the other hand, all parameters of Hardening Soil-Brick model can be derived based on CPTu and certain assumptions. Particularly well defined formulas can be found for parameters of normally consolidated sands.
This paper deals with the probabilistic modelling of a triple-anchored diaphragm wall, with its geometry assumed to be identical to one of the Berlin sand wall benchmarks (Schweiger 2002). The study assumes only one sand layer, focusing on its spatial variability using RFEM. The probability distribution cross-correlation coefficient and

vertical SOF for random fields describing Q_{tn} and F_r were identified based on CPTu tests of normally consolidated sand from central part of Poland. The horizontal SOF was assumed to be infinite. The Hardening Soil-Brick model was adopted for the soil medium. Its parameters in each soil modelling element were determined by known transformation formulas and local Q_{tn} and F_r values assigned to this element in a given realisation. N=1000 Monte Carlo simulations were considered. The paper presents the obtained probability characteristics of the results, namely the maximum displacement and bending moment in the wall as well as force in the upper anchor.

2 CPTu results and random field modelling

2.1 Identification of the field parameters

Soil variability was modelled by a random field of normalised CPTu parameters, i.e. Q_{tn} and F_r. The parameters of the random field describing these quantities were identified from CPTu tests of sand from central part of Poland. The measured values of Q_{tn} and F_r for that layer (averaged every 5cm) is presented in Robertson's nomogram (Robertson and Cabal, 2015) in Fig 1. As seen, the tested sand is mostly normally consolidated.

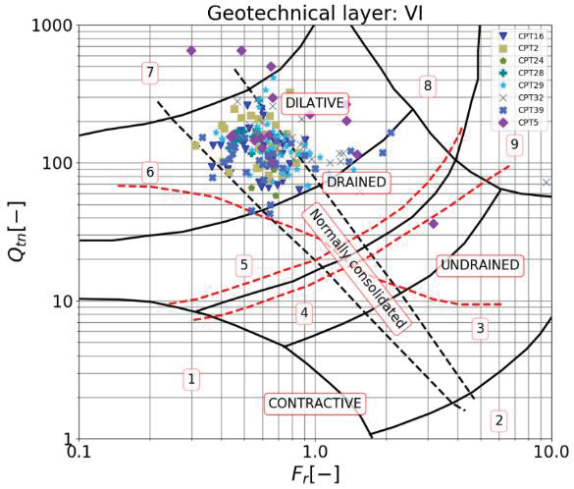

Figure 1. Q_{tn} and F_r values in Robertson's nomogram (Robertson and Cabal, 2015)

In a first step, the point probability distributions of these two quantities were identified. Since the range of those parameters is bounded as a probabilistic model the bounded distribution of the hyperbolic tangent (Fenton and Griffiths 2008, Kawa and Puła 2020) was accepted. The probability density function (PDF) of this distribution can be written analytically using following formula:

$$\mathrm{PDF}(t)=\begin{cases}\dfrac{\sqrt{\pi}\,(b-a)}{\sqrt{2}s\,(t-a)(b-t)}\exp\left\{-\dfrac{1}{2s^2}\left[\pi\ln\left(\dfrac{t-a}{b-t}\right)-m\right]^2\right\}, & t\in(a,b)\\ 0, & t\notin(a,b)\end{cases} \tag{1}$$

where m and s (as well as a and b denoting upper and lower bound of the support) are the distribution parameters. This distribution can also be obtained by a simple transformation of the standard normal distribution X_0.:

$$Y=a+\frac{1}{2}(b-a)\left[1+\tanh\left(\frac{m+sX_0}{2\pi}\right)\right] \tag{2}$$

The resulting fits of this distribution to the histograms of Q_{tn} and F_r values of the investigated layer are shown in Figs 2a and 2b, respectively. These fits were obtained for the following parameters: for Q_{tn} a=0 b=310, m=-1.594, s=2.075 and for F_r a =0.1, b=2.5, m=-3.885, s=1.373, respectively.

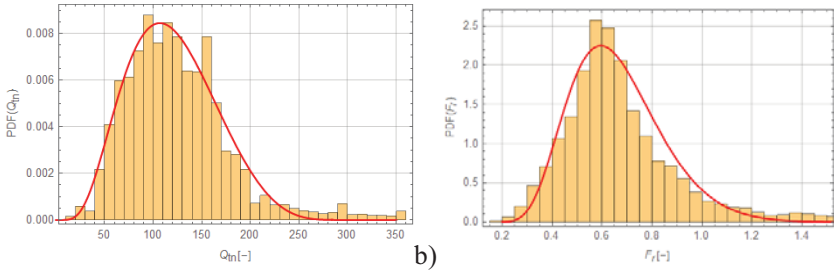

a) b)

Figure 2. Fit of tanh distribution in histograms of normalized CPTu measurements Q_{tn} and F_r

The cross-correlation coefficient ρ_{cross} between Q_{tn} and F_r values was also identified as 0.22.
In a second step, the vertical SOF for the examined layer based on the Q_{tn} values was determined. The method of moments was used (Cami 2020). The weak global linear trend with depth, defined as 3.37*z+97.12, was subtracted from the parameter value. Then, for each CPTu profile the empirical autocorrelation function was determined and the mean function was fitted with assumed Gaussian model:

$$\rho(\tau) = \exp\left\{-\pi\left(\frac{\tau}{\theta}\right)^2\right\} \tag{3}$$

The resulting SOF value was 0.482m. Due to the large distance between individual CPTu profiles the horizontal SOF was not determined.

2.2 Generation of the fields

Based on the identified values the random fields modelling Q_{tn} and F_r were generated. The Gaussian autocorrelation function (2D version of Eq. 3) with vertical SOF θ_z rounded to 0.5m and horizontal scale of fluctuation θ_x equal to infinity was assumed. Adoption of infinite horizontal SOF results in the greatest variability of boundary problem results (cf. Kawa et al. 2021) and thus should be considered as a conservative approach.
For generation of the fields the 2D FSM (Jha and Ching 2012), which generates locally averaged field values for arbitrary irregular rectangular mesh (all rows and columns can be of different width, but their number need to be constant) was employed. Due to the local variations of the grid density in the boundary value problem in a situation where e.g. two rows (or columns) of elements in one part of the mesh correspond to one row (or column) of elements in another part of the mesh, for the larger elements still two values was generated (to satisfy conditions of the FSM generator) and after that the mean of these two values was assign to the element. The cross-correlation between the parameters was also considered.
The following procedure was adopted. First, two independent Gaussian fields were generated using FSM assuming a finer mesh across the whole domain (also in parts where coarser mesh was used in the boundary value problem). Then every two corresponding values of the two fields was correlated by multiplying their column vector by the Cholesky's decomposition of the cross-correlation matrix. The latter can be written as

$$R_{cross} = \begin{bmatrix} 1 & \rho_{\text{cross}} \\ \rho_{\text{cross}} & 1 \end{bmatrix} \tag{4}$$

Subsequently the values of the correlated standard fields where transformed to Q_{tn} or F_r values, respectively using Eq.2 with parameters identified previously. Finally in coarser part of the mesh the appropriate means of the two values obtained assuming finer mesh, were calculated.

3 Numerical model of an anchored diaphragm wall

The anchored diaphragm wall case study is based on the benchmark of a deep excavation in Berlin sand (Schweiger 2002). Geometry of the excavation (depth 16.8m), diaphragm wall (length 32m, thickness 80 cm), highly impermeable barrier (thickness 2m), soil anchors, with their free/full lengths and initial prestress forces, position of groundwater water table and different discretization zones (A, B) are shown in Fig.3. Contrary to the original data setup anchors in the first row are 21.8m long instead of 19.8m. Another modification concerns the offset between current free water table and bottom of excavation which is 3m. The computational domain is discretized here using a unit slice of 8-node 3D EAS continuum and 8 node solid-shell elements therefore anchors cross section area and prestress force must be divided by the spacing value (2.3m in the first row and 1.35m in the second and third row of anchors). The major difference between the benchmark and current study is concerned with subsoil properties that are derived from random values of dimensionless Q_{tn} and F_r parameters.
The approximate grid size in zones of dense mesh (zones A in Fig.4) is 0.43m x 0.245m x 1m while in zones of a coarser mesh (zones B) grid size is approximately 0.86m x 0.49m x 1m. Continuity of the displacement and pore water pressures along the interface between dense and coarse meshes is preserved using mesh tying method. Anchor elements in the zone of free length are represented by a single 2-node elastic truss element while in the fixed zone extra discretization is enforced (using an exact intersection of the fixed anchor zone line segment with the 3D continuum mesh) and extra nodes are attached to the background mesh using kinematic constraints to

enforce deformation continuity. A frictional Coulomb's contact interface is added between the wall and subsoil. Friction angle in the interface is set as relative with respect to the friction angle in adjacent subsoil assuming that $\tan(\phi_i) = 0.66\tan(\phi_{soil})$. In this study the simplest computational approach is used in which nonlinear subsoil behavior is represented by the Hardening Soil-Brick model with random properties while the reinforced concrete wall is an elastic shell structure with deterministic properties $E = 30000$ MPa, $\nu = 0.2$ and $\gamma = 25$ kN/m^3. All simulations were run using ZSoil v2020 software (ZSoil 2020). Due to high permeability of sands the uncoupled two-phase formulation was used. In this formulation the soil-water retention curve (SWRC) for the partially saturated medium is described using simplified version ($n = 2$, $m = 1/2$) of the van Genuchten's law.

$$S = S_r + (1 - S_r) / \left(1 + \left(\alpha\, p / \gamma^f\right)^2\right)^{1/2} \tag{5}$$

For sands residual saturation ratio $S_r = 0$, $\alpha \approx 10$ [1/m] and seepage coefficient $k = 10^{-4}$ [m/s]. In the zone of a highly impermeable barrier $S_r = 0.1$, $\alpha \approx 0.2$ $\left[\frac{1}{\mathrm{m}}\right]$ and $k = 10^{-10}$ [m/s] (here SWRC parameters are not meaningful due to full saturation in this zone).

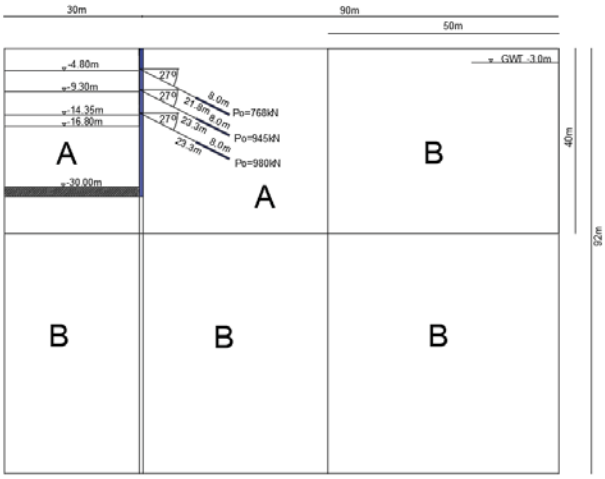

Figure 3. Engineering draft of the excavation

4 Deriving HS-Brick model parameters from random pairs (Q_{tn}, F_r)

The full set of material parameters required by the HS-Brick model consists of four groups i.e. stiffness, characterized by the unloading-reloading stiffness reference modulus $E_{\mathrm{ur}}^{\mathrm{ref}}$, secant stiffness modulus E_{50}^{ref}, power exponent *n*, Poisson's ratio *v*, oedometric tangent stiffness modulus E_{oed} set for a given vertical stress σ_v, stiffness reference modulus at very low strains E_0^{ref} and equivalent strain value $\gamma_{0.7}$ for which secant stiffness modulus E_s drops down to $0.7E_0$, then strength and dilatancy, represented by the friction angle ϕ, cohesion *c* and dilatancy angle ψ, stress history, represented by the OCR or the preoverburden pressure value.

In this study we assume that sandy subsoil is normally consolidated. It is obvious that with the two CPT dimensionless parameters Q_{tn} and F_r it is not possible to calibrate all aforementioned HS-Brick model parameters. Therefore the additional knowledge obtained from other experiments like the triaxial, oedometric or resonant columns tests, must be included. To simplify the study we assume that the Poisson's ratio is constant *v*=0.2, OCR=1, the well-known formula for K_0^{NC} is used $K_0^{\mathrm{NC}} = 1 - \sin\phi$, $\gamma_{0.7} = 0.0002$, $c = 0$ kPa and $\gamma_d = 15.0$kN/m^3 (dry unit weight). Further assumptions concerning fixed relations between pairs of stiffness moduli are as follows: $E_0^{\mathrm{ref}}/E_{\mathrm{ur}}^{\mathrm{ref}} = 2$, $E_{\mathrm{ur}}^{\mathrm{ref}}/E_{50}^{\mathrm{ref}} = 2.5$ and $E_{\mathrm{oed}} = E_{50}^{\mathrm{ref}}$ for $\sigma_v = \sigma^{\mathrm{ref}}/K_0^{\mathrm{NC}}$ (σ^{ref}=100 kPa). As far as stiffness moduli are concerned the only direct link between the HS-Brick model parameters and the correlation formulas known for the CPTU test is through the stiffness modulus E_0. A standard stiffness modulus *E* that can be estimated from the CPTU test results is the one bound by the E_{ur} and E_{50}, therefore its value can only be used to verify the assumption on assumed ratios between $E_0^{\mathrm{ref}}/E_{\mathrm{ur}}^{\mathrm{ref}}$ and $E_{\mathrm{ur}}^{\mathrm{ref}}/E_{50}^{\mathrm{ref}}$. In the general procedure designed to set random material properties at each soil element for a given pair (Q_{tn}, F_r), and known effective/total vertical stresses, σ'_{v0} and σ_{v0}, one can compute the soil behavior type index I_c (p_a =100 kPa).

$$I_c = [(3.47 - \log Q_{tn})^2 + (\log F_r + 1.22)^2]^{0.5} \quad (6)$$

Then from the Q_{tn} and σ'_{v0}, σ_{v0} one can easily derive the corrected cone resistance q_t. Based on the q_t and I_c values power exponent n (same as m in the barotropy functions for the HS-Brick model, is derived

$$m = 0.381 I_c + 0.05\sigma'_{v0} / p_a - 0.15 \quad (7)$$

The peak friction angle is estimated using Bolton formula ($\phi_{cv} = 32^o$)

$$\phi = \phi_{cv} + 15.84 \log Q_{tn} - 26.88 \quad (8)$$

The dilatancy angle is set as

$$\psi = \phi - \phi_{cv} \quad (9)$$

The resulting high degree of non-associativity in the plastic flow rule may yield severe instabilities in the numerical solution especially for dense meshes. As the assumed grid size is rather small hence we assume that the maximum difference between the peak friction and dilatancy angles is limited to 28°. As the OCR=1 the resulting in situ K_0 coefficient can be computed using Jaky's formula

$$K_0 = K_o^{NC} = 1 - \sin\phi \quad (10)$$

The current unit weight is computed then as

$$\gamma = \gamma_d + n\, S\, \gamma_w \quad (11)$$

where n is the porosity ($n = 1 - \gamma_d / \gamma_s$ and γ_s =26.5 kN/m^3) and S is the current saturation ratio (note that in situ pore water pressure distribution is linear with suction pressure above groundwater table).
The Young's modulus E_0 is defined using the formula (Robertson and Cabal, 2015)

$$E_0 = 2(1+\nu)\ \gamma / g\ [10^{0.55 I_c + 1.68}(q_t - \sigma_{v0} / p_a)] \quad (12)$$

Then we assume that stiffness barotropy in the HS-Brick model is expressed by the mean effective stress

$$p' = \frac{1 + 2K_0}{3}\sigma'_{v0} \quad (13)$$

which yields the following reference modulus value

$$E_0^{ref} = E_0 / \left(\frac{p'}{\sigma^{ref}}\right)^m \quad (14)$$

The remaining reference stiffness moduli $E_{\mathrm{ur}}^{\mathrm{ref}}$, E_{50}^{ref} are computed then based on the E_0^{ref} value and assumed ratios $E_0^{\mathrm{ref}}/E_{\mathrm{ur}}^{\mathrm{ref}} = 2$, $E_{\mathrm{ur}}^{\mathrm{ref}}/E_{50}^{\mathrm{ref}} = 2.5$, $E_{oed} = E_{50}^{\mathrm{ref}}$ at vertical stress $\sigma_v = \sigma_{ref}/K_0^{NC}$.

4 Results of simulations

The results from 1000 implementations were collected and are presented below as histograms. The histogram of the maximum wall displacement is shown in Fig 4a., histogram of the maximum moment in Fig 4b. and histogram of maximum force in the upper anchor Fig 4c. In all cases the obtained means, standard deviations and coefficients of variation are summarised in Table 1.

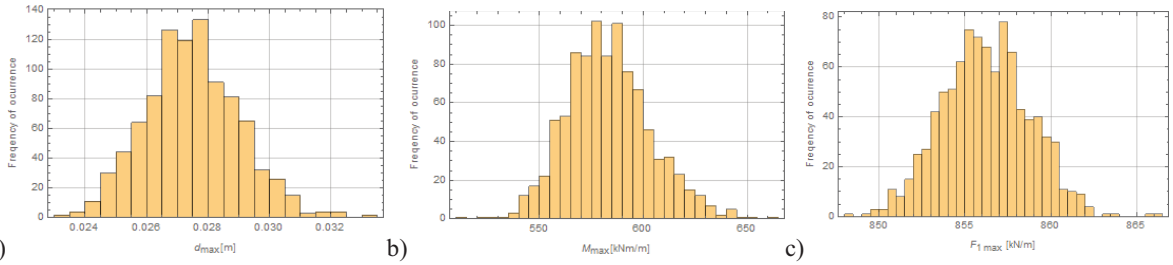

a) b) c)

Figure 4. Histograms of a) maximum displacement b) maximum bending moment c) maximum force in anchor

As seen, the maximum wall displacement is characterized by the highest coefficient of variation. In the case of torque, the ratio is much smaller, but it is still significant. The maximum force in the anchor varies little between

the simulations. These results show that even if adequate reinforcement is used for the wall (and thus the bending moment strength for the wall is not a decisive factor) in some cases the wall may fail due to significant displacement (if displacements of the wall are limited to e.g. 3cm).
The significant moment values also suggest the possibility of exceeding another serviceability limit state, i.e. the width of crack opening. This condition can be also important for risk assessment or reliability based design of wall, however it was not analysed in the present study.

Table 1. Statistical moments of resulting quantities.

Tested quantity	Mean	Standard deviation	Coefficient of variation
Maximum displacement	$2.75*10^{-2}$ m	$0.153*10^{-2}$ m	0.055
Maximum moment	583.2 kNm/m	20.3 kNm/m	0.035
Maximum force in upper anchor	856.2 kN/m	2.55 kN/m	0.003

5 Conclusions

In this study, an anchored diaphragm was modelled taking into account the spatial variability of the sandy subsoil. The HS-Brick model was used to describe the soil. The spatial variability of the normally consolidated sand was modelled by identified random fields describing the normalized CPTu parameters, i.e. Q_{tn} and F_r. Based on the generated values in each realization, all the parameters of the adopted model were determined. Probabilistic modelling was based on N=1000 Monte-Carlo simulations. The statistical characteristics of results, namely maximum wall displacement, maximum bending moment and force in the upper anchor, are presented in in the paper.
The maximum displacement of considered anchored wall in a spatially varying medium is characterised by a rather large coefficient of variation, app. 5%. Smaller values for the coefficient of variation (app. 3.5%) apply to maximum bending moments. According to the calculations, the forces in the anchor varied little between simulations. This shows that the serviceability limit state is quite important in the case under consideration, especially as it may determine the safety of the structure behind the wall.
The complete design of the structure was not analysed in this study although it is required to verify both the ULS and all SLS (wall deflections and maximum crack opening) limit states. Only the design of the wall with respect to the given allowable failure probability of the respective limit states, i.e. ultimate bearing capacity of the reinforced concrete cross section and anchors (ultimate), maximum crack opening (serviceability), and maximum displacements (serviceability) can be considered a complete reliability design.

References

Cami, B., Javankhoshdel, S., Phoon, K. K., & Ching, J. (2020). Scale of fluctuation for spatially varying soils: estimation methods and values. ASCE-ASME Journal of Risk and Uncertainty in Engineering Systems, Part A: Civil Engineering, 6(4), 03120002.

Fenton G. A., Griffiths D. V. (2003). *Bearing capacity prediction of spatially random c−ϕ soil*. Canadian Geotechnical Journal. 40. 54-65. 10.1139/t02-086.

Fenton, G. A., & Griffiths, D. V. (2008). Risk assessment in geotechnical engineering (pp. 381-399). Hoboken, New Jersey: John Wiley & Sons, Inc..

Griffiths D. V & Fenton G. A. (1993) Seepage beneath water retaining structures founded on spatially random soil. Geotechnique; **43**(6): 577-587.

Griffiths, D. V., & Fenton, G. A. (2004). Probabilistic slope stability analysis by finite elements. Journal of geotechnical and geoenvironmental engineering, 130(5), 507-518.

Jha S., Ching J. (2012). *Simulating Spatial Averages of Stationary Random Field Using the Fourier Series Method*, Journal of Engineering Mechanics. 139. 594-605. 10.1061/(ASCE)EM.1943-7889.0000517.

Kawa, M., Puła, W. (2020). *3D bearing capacity probabilistic analyses of footings on spatially variable c–φ soil*. Acta Geotech. 15, 1453–1466.

Kawa M., Puła W., Truty A. (2021). *Probabilistic analysis of the diaphragm wall using the hardening soil-small (HSs) model*. Engineering Structures. 232. 111869. ISSN 0141-0296.

Luo Z, Li Y, Zhou S, Di H. (2018) Effects of vertical spatial variability on supported excavations in sands considering multiple geotechnical and structural failure modes. Comput Geotech;95:16–29.

Robertson, P. K., & Cabal, K. L. (2015). Guide to cone penetration testing 6th Edition. Gregg Drilling & Testing. Inc. 6th Edition, Signal Hill, California.

Schweiger, H. F. (2002). Benchmarking in geotechnics. Part 1: Results for benchmarking; Part 2: Reference solution and parametric study. Institute for Soil Mechanics and Foundation Engineering, Graz University of Technology, Austria.

Sert S., Luo Z., Xiao J., Gong W., Juang C. H. (2016). *Probabilistic analysis of responses of cantilever wall-supported excavations in sands considering vertical spatial variability*. Computers and Geotechnics. 75. 182-191. ISSN 0266-352X

User manual ZSoil.PC v2020. *Soil, Rock and Structural Mechanics in dry or partially saturated media*. ZACE Services Ltd, Software Engineering, Lausanne, Switzerland, 1985-2020.